Chemical Science

EDGE ARTICLE

View Article Online
View Journal | View Issue

Cite this: *Chem. Sci.*, 2014, **5**, 3287

Spectroscopic determination of crystal field splittings in lanthanide double deckers†

R. Marx,[a] F. Moro,‡[b] M. Dörfel,[a] L. Ungur,[c] M. Waters,[b] S. D. Jiang,[d] M. Orlita,[e] J. Taylor,[f] W. Frey,[g] L. F. Chibotaru*[c] and J. van Slageren*[a]

Received 12th March 2014
Accepted 22nd May 2014

DOI: 10.1039/c4sc00751d

www.rsc.org/chemicalscience

We have investigated the crystal field splitting in the archetypal lanthanide-based single-ion magnets and related complexes $(NBu_4)^+[LnPc_2]^-\cdot 2dmf$ (Ln = Dy, Ho, Er; dmf = *N*,*N*-dimethylformamide) by means of far infrared and inelastic neutron scattering spectroscopies. In each case, we have found several features corresponding to direct crystal field transitions within the ground multiplet. The observation of three independent peaks in the holmium derivative enabled us to derive crystal field splitting parameters. In addition, we have carried out CASSCF calculations. We show that exploiting the interplay of CASSCF calculation (for the composition of the states) and advanced spectroscopic measurements (for accurate determination of the energies) is a very powerful approach to gain insight into the electronic structure of lanthanide-based single-molecule magnets.

Introduction

The use of lanthanide ions for preparing novel mono- or polynuclear clusters that display slow magnetization dynamics (single-molecule magnets, SMMs) has enjoyed exponentially increasing interest during the last decade.[1] This interest arose, because Arrhenius fits of the temperature dependence of the relaxation time often yield much larger effective energy barriers for lanthanide than for (polynuclear) transition metal based systems. Thus the highest reported energy barrier is only 84 K for transition metal cage complexes, while values of almost 1000 K have been reported for lanthanide-based systems.[2–4] In spite of these much larger energy barriers, most lanthanide complexes show virtually no magnetic hysteresis, and, indeed, slow relaxation is often observed only in applied dc magnetic fields. Clearly, for the envisaged application of magnetic data storage, magnetic bistability is an essential prerequisite. A second issue is that the data points in the Arrhenius plot of ln τ *vs.* T^{-1} (τ, T are the relaxation time and temperature, respectively) typically lie on a straight line over a much smaller range of relaxation times than observed for transition metal cage compounds. Indeed, of the possible relaxation mechanisms, including direct relaxation, quantum tunnelling, Raman relaxation and Orbach relaxation, only the last has an exponential temperature dependence.[5] The Orbach process of spin relaxation is a two-phonon process that proceeds *via* a real intermediate state, which is an excited crystal field state in lanthanide ions.[5] Hence, the role of the crystal field in the magnetization relaxation is unclear,[6–8] and very few experimental data on the direct determination of the crystal field splitting in lanthanide-based SMMs have been reported.[9–13] From the theoretical side, currently, two avenues are being pursued. First of these is the computationally convenient semi-empirical method based on crystal field parametrisation.[14] Secondly, *ab initio* CASSCF-based methods, which are computationally more challenging, but do not involve fitting to experimental data, have been very successful.[15] In order to assess the correctness and predictive powers of these theoretical methods, as well as improvement of the same, spectroscopic data are indispensable. Experimental information on the crystal field (CF) splitting in lanthanide compounds is typically obtained from optical spectroscopies, such as electronic absorption, luminescence, or magnetic circular dichroism spectroscopies, which allow direct determination of CF splittings of ground and excited multiplets by observation of the splittings of peaks due to ff

[a]*Institut für Physikalische Chemie, Universität Stuttgart, Pfaffenwaldring 55, 70569 Stuttgart, Germany. E-mail: slageren@ipc.uni-stuttgart.de*

[b]*School of Chemistry, University of Nottingham, University Park, Nottingham, NG7 2RD, UK*

[c]*Division of Quantum and Physical Chemistry, Katholieke Universiteit Leuven, Celestijnenlaan 200F, 3001 Leuven, Belgium. E-mail: Liviu.Chibotaru@chem.kuleuven.be*

[d]*1. Physikalisches Institut, Universität Stuttgart, Pfaffenwaldring 57, 70569 Stuttgart, Germany*

[e]*Laboratoire national des champs magnétiques intenses, CNRS-UJF-UPS-INSA, 38042 Grenoble Cedex 9, France*

[f]*ISIS, Rutherford Appleton Laboratory, Harwell Oxford, UK*

[g]*Institut für Organische Chemie, Universität Stuttgart, Pfaffenwaldring 55, 70569 Stuttgart, Germany*

† Electronic supplementary information (ESI) available: Details on synthesis, crystallography and calculations. Experimental magnetometry, INS and FIR data, further spectral simulations, outputs from CASSCF calculations. CCDC [996593–996595]. For ESI and crystallographic data in CIF or other electronic format see DOI: 10.1039/c4sc00751d

‡ Present address: School of Physics, University of Nottingham, University Park, Nottingham, NG7 2RD, UK.

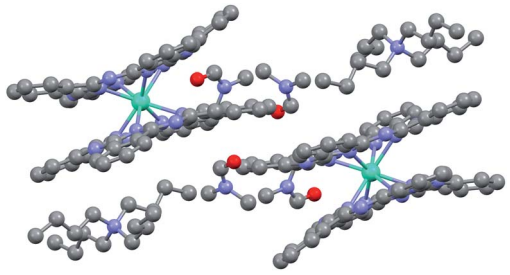

Fig. 1 Crystal structure of the compounds $(NBu_4)^+[LnPc_2]^-\cdot 2dmf$ with carbon in grey, nitrogen in blue, lanthanide ions in green and oxygen in red. The inversion centre is in the middle of the image.

transitions.[12,13,16,17] However, for the first and now archetypal lanthanide SMMs, the complexes $[LnPc_2]^{+/0/-}$ (Tb, Dy, Ho; H_2Pc = phthalocyanine),[18] such data are not accessible. This is because the UV/Vis/NIR region of the electromagnetic spectrum is dominated by the phthalocyaninate ligand, whose absorptions are many orders of magnitude stronger than those due to ff transitions. Hence, other experimental methods have to be resorted to, including inelastic neutron scattering (INS),[10,11,17,19,20] and far infrared (FIR) spectroscopies.[21,22]

Here we present an experimental study of the crystal field splitting of the compounds $(NBu_4)^+[LnPc_2]^-\cdot 2dmf$ (**1Ln**, Ln = Dy, Ho, Er; dmf = *N*,*N*-dimethylformamide, Fig. 1), of which the former two are SMMs. We did not include the terbium derivative, because no spectral features in the accessible energy range are expected. We employ FIR and INS spectroscopies to directly observe crystal field transitions within the ground Russell-Saunders multiplets. In addition, we report CASSCF-based calculations of the CF splittings. We derive CF splitting parameters from the measurements and compare experimental and theoretical electronic structures.

Results and discussion

Structures and symmetries

Upon recrystallization from dmf with added hydrazine, the complexes $(NBu_4)^+[LnPc_2]^-\cdot 2dmf$ of the later lanthanides (Gd–Yb) all crystallize in the space group $P\bar{1}$, where the inversion centre is between two molecules (Fig. 1 and Table S1†).[23] Hence, the site symmetry is C_1. Describing the crystal field splitting by means of the CF spin Hamiltonian, written in terms of extended Stevens operators,[16]

$$\mathscr{H}_{CF} = \sum_{k=2,4,6} \sum_{q=-k}^{+k} B_k^q \hat{O}_k^q \qquad (1)$$

up to 27 CF parameters could be included. Fortunately, the idealized symmetry is very close to D_{4d}. Thus, for **1Ho**, the distances between metal ion and coordinating nitrogen atom are all virtually the same at 2.41 ± 0.01 Å. The angle between the two planes defined by the four coordinating nitrogen atoms of each ligand is 0.59°, where 0° would be expected for fourfold symmetry. The skew angles between the two ligands, defined as the angles between the two planes formed by Ho and two of the coordinating nitrogens of one ligand and Ho and two of the coordinating nitrogens on the other ligand are 45 ± 1°, where for D_{4d} 45° would be expected. These parameters are very similar to those published for $(NBu_4)^+[HoPc_2]^-\cdot H_2O$ (Table S2†).[24] In D_{4d} symmetry there are only three CF-parameters, and this is the Hamiltonian that we have used for fitting of the experimental data of **1Ho**:

$$\mathscr{H}_{CF} = B_2^0\hat{O}_2^0 + B_4^0\hat{O}_4^0 + B_6^0\hat{O}_6^0 \qquad (2)$$

For **1Dy** and **1Er** an insufficient number of peaks was observed to allow direct determination of crystal field parameters, given that for three parameters at least three transition energies need to be determined (see below).

Direct current (dc) and alternating current (ac) magnetic susceptibility

The magnetic susceptibilities of powder samples for all complexes were measured, the results for **1Dy**, **1Ho** and **1Er** are shown in Fig. 2. The $\chi_m T$ values at room temperature (13.58, 13.76 and 11.63 $cm^3\ K\ mol^{-1}$, for **1Dy**, **1Ho** and **1Er**, respectively) are very close to values expected for the Russell-Saunders ground multiplets for these ions in the absence of crystal field splitting (14.17, 14.07, 11.48 $cm^3\ K\ mol^{-1}$),[25] and quite close to those previously published.[26] The decrease in $\chi_m T$ values towards lower temperatures is due to depopulation of the microstates of the ground multiplets ($^6H_{15/2}$, $^5I_8$, $^4I_{15/2}$, for Dy, Ho, Er, respectively) that are split due to the crystal field of the surrounding ligands.

At the temperatures ($T > 1.8$ K) and frequencies ($\nu < 1500$ Hz) available to use, only **1Dy** displays measurably slow relaxation of the magnetization (Fig. S1†). The temperature dependence of the relaxation time τ at a given temperature is extracted from the maxima of the out-of-phase component of the ac susceptibility (χ''), where the following relation holds $\tau = (2\pi\nu_{ac})^{-1}$. The

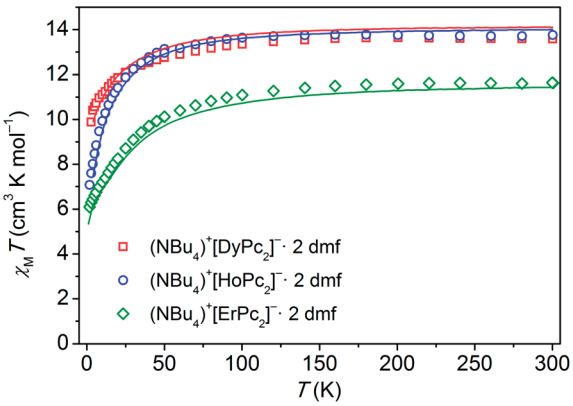

Fig. 2 DC magnetic susceptibility temperature product ($\chi_m T$) as a function of temperature for **1Dy**, **1Ho**, and **1Er** (symbols), measured with a static magnetic field of 1000 Oe, as well as simulations based on crystal field parameters obtained from CASSCF/RASSI calculations projected on an effective angular momentum ground multiplet (lines). The theoretical energies were scaled by the following factors 0.68 (**1Dy**), 1.31 (**1Ho**), or 1.27 (**1Er**), see text.

effective energy barrier towards relaxation of the magnetic moment was determined from the Arrhenius equation ($\tau = \tau_0 \exp(\Delta E/kT)$) to be $\Delta E = 34 \pm 1$ cm^{-1} This value is very similar to that obtained by Ishikawa on an unknown phase of the material ($\Delta E = 31$ cm^{-1}).[27]

$(NBu_4)^+[DyPc_2]^- \cdot 2dmf$ (1Dy)

We have studied **1Dy** by means of both far-infrared (FIR) and inelastic neutron (INS) spectroscopies (Fig. 3 and S2–S6†). The normalised FIR spectra display distinct zero field features (normalised transmission < 1) at 32.8 cm^{-1}, while application of an external field shifts the spectral density to higher energies (normalised transmission > 1). In the INS spectrum, one peak, whose width clearly exceeds the instrumental resolution, is observed at 37 cm^{-1}. The apparent discrepancy between the two values is due to the field normalisation procedure in the FIR spectra: The shift of the spectral density to higher frequencies on increasing the field leads to a shift of the frequency position of the minimum in the normalised transmission spectra to lower frequencies. The disappearance of the 37 cm^{-1} INS-peak at higher temperatures, as well as the essentially flat Q-dependence of the scattering intensity at low Q (Fig. S4†) both indicate its magnetic origin. We assign the peaks in both FIR and INS spectra to a single transition from the ground Kramers' doublet. The observed transition energy of *ca.* 37 cm^{-1} agrees rather well with the energy gap (35 cm^{-1}) between the $|m_J\rangle = |\pm 13/2\rangle$ ground and $|\pm 11/2\rangle$ excited Kramers' doublets, predicted by Ishikawa *et al.*,[26] on the basis of fits of powder susceptibility measurements (Fig. 4). Recent calculations, based on an effective point charge parameterisation of crystal field theory also yield a very similar lowest energy gap of 42 cm^{-1} (Fig. 4).[14] Interestingly, the ground and excited Kramers' doublets are inverted. The excitation energy (37 cm^{-1}) is higher than the energy barrier towards relaxation of the magnetic moment of 34 cm^{-1}, found from an Arrhenius fit of the temperature dependence of the relaxation time determined by ac susceptibility measurements. Here we now demonstrate that there is indeed a crystal field state close to the experimentally observed energy barrier. Hence, it is likely that the Orbach process, which is by no means to be automatically invoked to describe spin relaxation in lanthanide ions,[5] indeed plays a role in **1Dy**. The discrepancy between the two values indicates additional processes must play a role in the spin relaxation in **1Dy**. At higher energies, additional features are observed (Fig. S5 and S6†), whose attribution is more difficult since at higher energy transfers, the diagnostic low momentum transfer range is not experimentally accessible. The fact that similar high-energy features are observed for **1Ho** appears to preclude their attribution to CF transitions.

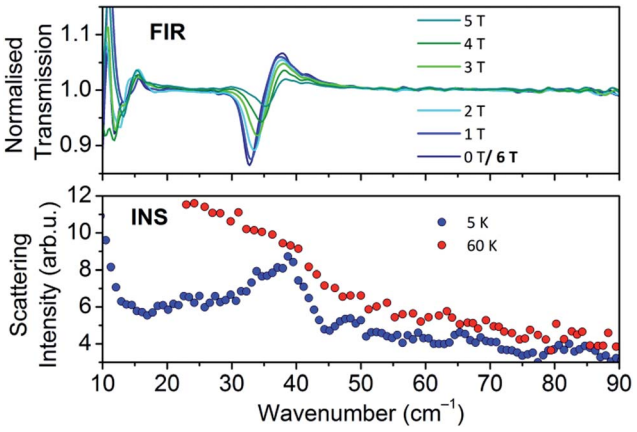

Fig. 3 (top) Far-infrared spectra normalised by division by the highest field (6 T) spectrum, recorded on a 10 mm pressed powder sample of **1Dy** at 10 K and different fields as indicated. (bottom) Inelastic neutron scattering spectrum recorded on *ca.* 1.8 g of **1Dy** at an incident neutron energy of 16 meV and temperatures as indicated, integrated over the momentum transfer range $0 \le Q \le 2$ Å^{-1}.

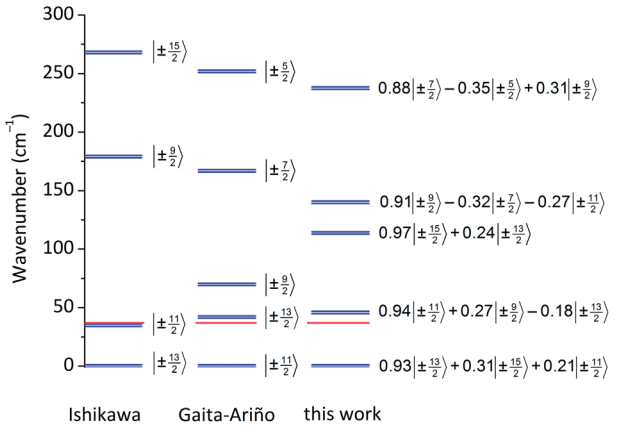

Fig. 4 Energy level diagram for **1Dy**, as derived by Ishikawa *et al.*,[26] Gaita Ariño *et al.*[14] and from CASSCF calculations reported here, with values rescaled by 0.68. The red line indicates the experimental transition frequency.

To further investigate the crystal field splitting we have carried out CASSCF calculations, using the experimental geometry, with the seven 4f-orbitals as active space.[15] These calculations find that the ground doublet is predominantly $|\pm 13/2\rangle$: $0.93|\pm 13/2\rangle + 0.31|\pm 15/2\rangle + 0.21|\pm 11/2\rangle$, while the first excited state is predominantly $|\pm 11/2\rangle$: $0.91|\pm 11/2\rangle + 0.34|\pm 9/2\rangle + 0.21|\pm 13/2\rangle$. (Tables S4–S6†) To assess the effect of charges further away (*i.e.* neighbouring molecules in the lattice) five layers of point charges were included into the calculation. This led to changes of the order of maximally 10% in the energies (Table S4†). The resulting calculated energy gap is 52.3 cm^{-1}, which is clearly larger than that found in experiment. On one hand, it must be noted that the lowest energy gap decreases from 75.6 to 52.3 cm^{-1} going from a double zeta to triple zeta basis set, and hence for a bigger basis set it can be expected that this trend continues and a splitting closer to the experimental one would be obtained. Unfortunately, the use of a quadruple basis set is precluded by available computational resources, given the large size of the system. On the other hand, however, there is a potential experimental reason for this discrepancy, because the calculations were based on the crystal structures determined at around 100 K, and the structure may be slightly different at the temperatures employed for the FIR

measurements. We have therefore carried out further calculations on **1Dy**, where we have varied the interligand distance by ±0.05 Å (Table S7†). These calculations show that the changes in the energies are of the order of the discrepancies between calculated and experimental data. Also the direction of the energy shifts does not depend monotonously on the interligand distance. The calculated *g*-tensors of the lowest doublet do not vary greatly, showing that the wavefunctions do not change significantly. Unfortunately, for the systems under study here, no low-temperature crystal data are available. The FIR spectra and dc susceptibility can be simulated well using the CF parameters found in the CASSCF calculations (Fig. 2 and S7–S9†). Here we have used a semi-empirical scaling factor of 0.68 to account for effects of the necessarily limited size of the employed basis sets, unaccounted dynamical correlation and possible deviations of low-temperature structure from the high-temperature one used in the calculations. Simulations based on CF parameters reported in literature are given for comparison (Fig. S8†).[14,26]

$(NBu_4)^+[HoPc_2]^- \cdot 2dmf$ (1Ho)

Fig. 5 and S10† display high-resolution (0.12 cm^{-1}) FIR spectra up to 100 cm^{-1}, while slightly lower resolution (1 cm^{-1}) spectra up to 200 cm^{-1} can be found in Fig. S11.† In both spectra, two distinct field-dependent peaks are observed at 19 ± 1 cm^{-1} and 53.3 ± 0.1 cm^{-1} (features pointing downward). At higher energies two further peaks are observed at 92 and 189 cm^{-1}. The temperature dependence of the FIR transmission spectra (Fig. 6) reveals two ground state features at 16 and 53.6 cm^{-1}, attributed to the same transitions as the field dependent peaks found at similar energies (Fig. 5, S10 and S11†). Peaks at the same energies are also observed in the INS spectra at low *Q* (Fig. 6 and S12–S14†). Ishikawa *et al.* find the lowest two CF excited quasi-doublets at 15 and 82 cm^{-1},[26] while Gaita-Ariño *et al.* find quasi-doublets at 25 and 31 cm^{-1}.[14] Interestingly, the temperature normalised FIR spectra (Fig. 6) show a peak pointing downward at 73 cm^{-1}, which must therefore involve increased spectral density at higher temperatures and is thus attributed to a transition from the first excited quasi-doublet at *ca.* 19 cm^{-1}. This attribution is corroborated by the observation of a small peak at 92 = 19 + 73 cm^{-1}.

Using the five crystal field transitions that we have observed, we can fit the three CF splitting parameters of eqn (2) to the corresponding energies (Table 1). In the fit procedure, we have assumed that the ground doublet is |±5> (note that the m_J functions are the eigenstates in D_{4d} symmetry). Inspection of Table 1 and Fig. S15† shows that the found parameters and resulting energy spectrum are quite different from those previously reported.[14,26] Intriguingly, all parameter sets give excellent fits of the magnetic susceptibility (Fig. S16†). This finding demonstrates that SQUID curves alone do not provide a reliable estimate of the CF splitting. Simulations (Fig. 5, S11 and S17†) of field- and temperature-normalised FIR spectra on the basis of the three derived CF parameters are in excellent agreement with the experimental data. In contrast, simulations based on CF parameters reported in literature are not nearly as

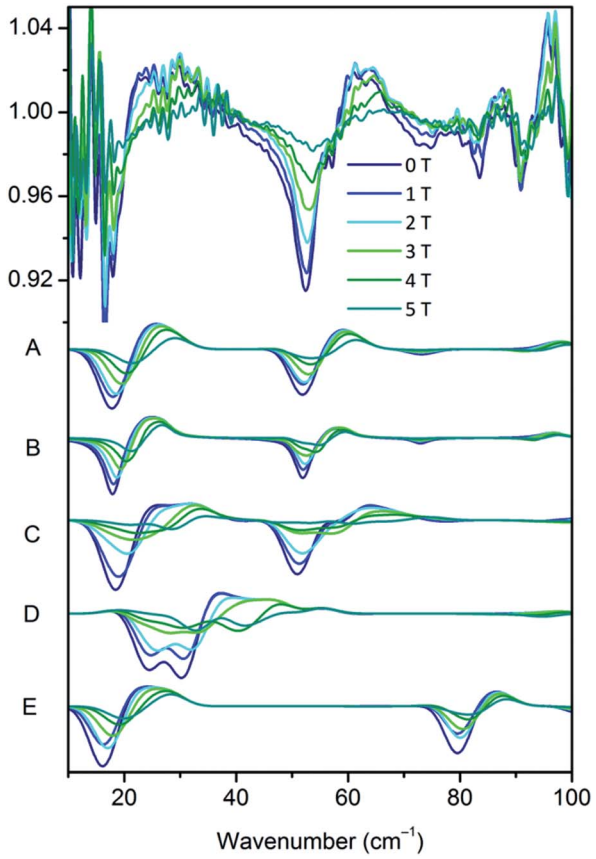

Fig. 5 Experimental FIR spectra recorded on a pressed powder sample of **1Ho** at 10 K and different magnetic fields as indicated, as well as simulations based on CF parameters (A) derived in this work assuming a |±5> ground doublet; (B) derived in this work assuming a |±6> ground doublet; (C) derived from CASSCF calculations, after rescaling of the energies of the states by 1.31; (D) reported by Gaita Ariño;[14] (E) reported by Ishikawa.[26]

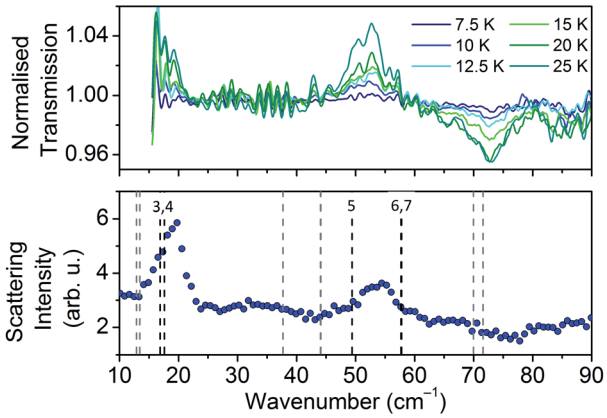

Fig. 6 (top) FIR spectra recorded on a pressed powder sample of **1Ho** at 0 T and different temperatures as indicated. All spectra have been normalised by division by the 5 K spectrum. (bottom) INS spectrum recorded on a 2.4 g powder sample of **1Ho** at 5 K and an incident neutron energy of $E_i = 12.5$ meV. The spectrum was integrated over a *Q* range of $0 \leq Q \leq 2$ Å^{-1}. Grey (black) dashed lines indicate the energy levels calculated by CASSCF methods for **1Ho** before (after) applying a scaling factor of 1.31.

Table 1 CF Splitting parameters (10^{-3} cm^{-1}) found in this work for **1Ho**, compared to reported values[14,26]

CF splitting term	This work GD = |±5>	This work GD = |±6>	Ishikawa	Gaita-Ariño
B_2^0	−257.8	−1244	−848.9	−446.7
B_4^0	6.00	7.90	6.50	5.90
B_4^4	—	—	—	0.788
B_6^0	−0.0305	−0.0116	−0.0543	−0.0200
B_6^4	—	—	—	0.0457

good, proving that spectroscopic data provide a much better means of assessing the correctness of CF parameters than magnetic data. However, assuming a |±6> rather than a |±5> ground doublet leads to almost equally good fits of susceptibility, magnetization and FIR (Fig. 5, S11 and S17†) demonstrating that FIR and INS spectroscopic measurements alone do not allow unequivocal determination of the eigenstates (Fig. S19†).

To gain further insight into the CF of **1Ho**, we have carried out CASSCF calculations similar to those performed for **1Dy**, again including five layers of point charges to simulate the effect of neighbouring molecules on the CF splitting, and also examining the effect of small distortions of the molecule on the energy spectrum (Tables S8–S11†). The energy level diagram obtained from the spectroscopic data (Fig. S15†) is very well reproduced by the CASSCF calculations assuming a scaling factor of 1.31. Again the direction of the scaling is in agreement with the energy changes going from a double to a triple zeta basis set. The calculations find that all microstates of the ground multiplet are heavily mixed. In part, this can be explained by the fact that holmium has an integer angular momentum quantum number and, not being subject to Kramers' theorem, twofold degeneracy is not necessarily maintained. In practice, the calculations find energy splittings of up to about 1 cm^{-1} between pairs of states that can be considered quasi-doublets. In addition, the compositions of the wavefunctions strongly depend on the choice of quantisation axis, where the highest g value direction of the ground microstate was chosen. This direction is quite far from the pseudo C_4 axis, something that is also found in single crystal SQUID measurements.[28] On the basis of the CF parameters derived from the CASSCF calculations excellent fits of the field- and temperature dependence of the FIR spectra as well as of the dc susceptibility are obtained (Fig. 2, 5, S11, S17 and S20–S22†).

$(NBu_4)^+[ErPc_2]^- \cdot 2dmf$ (1Er)

Fig. 7 displays field-normalised far-infrared spectra recorded on **1Er** (see also Fig. S23†). Two features can be observed, one located at 74 cm^{-1} in zero field, and a second one at low energies, which only appears within the spectral window at fields larger than 3 T. On application of an external magnetic field, a clear splitting of the high-frequency line can be observed. In accordance with the energy level diagram reported by Ishikawa *et al.*,[26] we assign the higher frequency zero-field peak to the

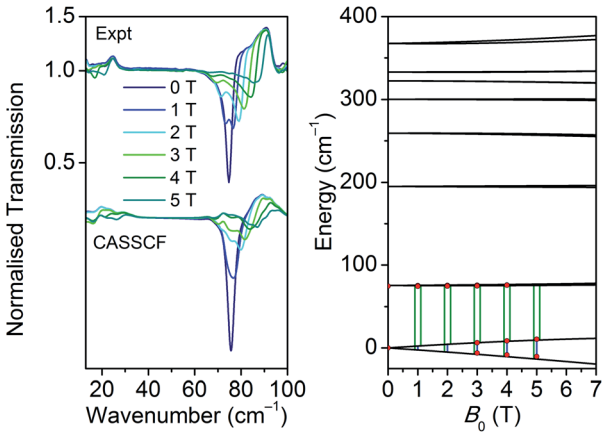

Fig. 7 (left, top) Experimental normalised FIR spectrum recorded on a powder sample of **1Er** at 10 K and different magnetic fields as indicated; (left, bottom) simulation on the basis of CF parameters derived from CASSCF calculations, assuming a scaling factor of 1.27. (right) Energy level diagram of **1Er** for magnetic fields perpendicular to the quantisation axis obtained by CASSCF calculations, with the same scaling factor, with the experimental transition energies as red symbols, the intra-ground-doublet transitions as blue and the inter-doublet transitions as green lines.

transition from the ground Kramers doublet |±1/2> to the first excited doublet |±3/2>, while the lower frequency peak is attributed to the transition |−1/2> to |+1/2> within the ground doublet. This assignment is supported by CASSCF calculations (Tables S12–S15†), according to which the ground doublet has 99% |±1/2> character, and the first excited doublet 98% |±3/2> character. The low frequency transition moves into the FIR spectral range at moderate fields, due to the large $g_\perp$ value of the ground doublet, which is expected to be $g_\perp \approx 9$ for a pure |±1/2> ground Kramers doublet. Indeed X-band EPR measurements (Fig. S24†) on **1Er** display a single resonance with $g_\perp = 9.59$ ($g_{||}$ was not observed). From the FIR measurements a g value for the ground doublet of $g = 9.01$ is obtained. Using this ground doublet g value and the observed splitting of the high-frequency line, the effective g value of the excited multiplet was determined to be almost zero, in accordance with the CASSCF calculations. The found zero-field energy gap between |±1/2> and |±3/2> of 74 cm^{-1} is clearly smaller than that derived by Ishikawa (102 cm^{-1}). The energy gap found from CASSCF calculations (Table S10†) is 58.7 cm^{-1}, which is rather smaller than the experimentally found transition energy, and a scaling factor of 1.27 is applied to match experimental and calculated transition energies. Use of the CF parameters derived from the CASSCF calculations (Table S11†) once more yield an excellent simulation of the experimental FIR spectra and susceptibility data (Fig. 2, 7 and S25†).

Experimental

The compounds **1Ln** were synthesized *via* a modified literature procedure (see ESI†).[29] Magnetic susceptibility measurements were carried out on a Quantum Design MPMSXL7 SQUID magnetometer. The diamagnetic correction of the measured

susceptibility was carried out by using the measured susceptibility of $(NBu_4)^+[YPc_2]^- \cdot 2dmf$, taking into account the difference in lanthanide ion through Pascal's constants.

Far infrared spectra were recorded on a Bruker 113v FTIR spectrometer equipped with a mercury vapour light source and an Infrared Laboratories pumped Si bolometer. Samples were attached to a sample holder inserted into an 8T Oxford Instruments Spectromag 4000 optical cryomagnet. The sample holder permitted *in situ* changing between an aperture and the sample, which allowed recording absolute transmission spectra. Samples were prepared as 10 mm pressed powder pellets, using *ca.* 25 mg of sample. To identify the relevant features, spectra were normalised by division by the spectrum at highest field or lowest temperature. The high frequency FIR spectrum ($T = 4.2$ K) of **1Ho** was recorded on a Bruker IFS 66v/s FTIR spectrometer with globar source, where the sample was placed inside an 11 T solenoid magnet, with a composite bolometer detector element located inside the magnet.

INS spectra were recorded on the MARI spectrometer at ISIS, Rutherford Appleton Laboratory, Didcot, UK. Samples were placed between cylindrical aluminium inner and outer cans to fully exploit the beam cross section, while preventing multiple scattering.

For crystal field calculations, as well as susceptibility and FIR simulations, the energy levels were calculated by means of the easyspin toolbox for Matlab.[30] These were then used to calculate the susceptibility by means of the Van Vleck equation. FIR spectra were calculated by convoluting transition energies and Boltzmann-weighted transition probabilities with the appropriate lineshape function.

CASSCF calculations were performed by using the MOLCAS 7.8 program package,[31] where the computational strategy has been described.[15] Spin free wavefunctions were calculated by means of CASSCF methods, using the seven 4f-orbitals as active space. The geometries were taking from the crystal structures and not optimised. Spin–orbit multiplets were calculated in a second step in a RASSI calculation. Finally, the obtained energies and wavefunctions were projected onto the ground Russell-Saunders multiplet to extract m_J compositions of the microstates and crystal field splitting parameters. The obtained energies were semi-empirically scaled by the following factors 0.68 (**1Dy**), 1.31 (**1Ho**), or 1.27 (**1Er**) to match the experimentally observed transition energies. Hence absolute accuracies were in the range 10–20 cm^{-1}. See ESI† for further details.

Conclusions

We have carried out some of the first inelastic neutron scattering and the first far infrared spectroscopic investigations of lanthanide-based single ion magnets. These techniques have allowed us to directly observe crystal field excitations within the ground Russell-Saunders multiplets. We have also calculated the electronic structures of these multiplets by means of CASSCF calculations. Through simulations of the magnetic susceptibility data as well as the spectra we find that susceptibility measurements do not allow discrimination between different crystal field parameter sets. We show that published crystal field parameters for the molecules under study do not always reproduce the true electronic structures. Hence spectroscopic data are indispensable for the refinement of crystal field theory parameterisations. Finally, we find that the agreement between experimental spectra and those calculated by CASSCF-based methods is astoundingly good. A scaling factor for the CASSCF energies was to take into account the effects of changes in molecular structure between the temperature at which these structures were determined, and the temperatures of the spectroscopic measurements. In addition, these scalings may account for the necessarily limited size of the employed basis sets, unaccounted dynamical correlation and possible deviations of low-temperature structure from the high-temperature one used in the calculations. We believe that the interplay of CASSCF calculations and spectroscopic methods such as far-infrared and inelastic neutron scattering spectroscopy will continue to prove very fruitful for the understanding of the electronic structures and hence the magnetic properties of lanthanide complexes, including single molecule magnets.

Acknowledgements

EPRSC (EP/G004757/1,2), DFG, COST CM1006 (STSM to MW), STFC (beamtime), EU (IEF 253980 to FM) and Alexander von Humboldt foundation (fellowship to SDJ) are all thanked for financial support. Prof. Martin Dressel (Stuttgart) is thanked for access to the FIR spectrometer and SQUID magnetometer. L. Ungur is a postdoc of the Flemish Science Foundation FWO-Vlaanderen, and gratefully acknowledges the support from Methusalem and INPAC grants of the KU Leuven.

Notes and references

1 D. N. Woodruff, R. E. P. Winpenny and R. A. Layfield, *Chem. Rev.*, 2013, **113**, 5110–5148.
2 C. J. Milios, A. Vinslava, W. Wernsdorfer, S. Moggach, S. Parsons, S. P. Perlepes, G. Christou and E. K. Brechin, *J. Am. Chem. Soc.*, 2007, **129**, 2754–2755.
3 C. R. Ganivet, B. Ballesteros, G. de la Torre, J. M. Clemente-Juan, E. Coronado and T. Torres, *Chem.–Eur. J.*, 2013, **19**, 1457–1465.
4 R. J. Blagg, L. Ungur, F. Tuna, J. Speak, P. Comar, D. Collison, W. Wernsdorfer, E. J. L. McInnes, L. F. Chibotaru and R. E. P. Winpenny, *Nat. Chem.*, 2013, **5**, 673–678.
5 A. Abragam and B. Bleany, *Electron Paramagnetic Resonance of Transition Ions*, Dover Publications, Inc., New York, 1986.
6 E. Lucaccini, L. Sorace, M. Perfetti, J.-P. Costes and R. Sessoli, *Chem. Commun.*, 2014, **50**, 1648–1651.
7 J. M. Zadrozny, M. Atanasov, A. M. Bryan, C.-Y. Lin, B. D. Rekken, P. P. Power, F. Neese and J. R. Long, *Chem. Sci.*, 2013, **4**, 125–138.
8 J.-L. Liu, K. Yuan, J.-D. Leng, L. Ungur, W. Wernsdorfer, F.-S. Guo, L. F. Chibotaru and M.-L. Tong, *Inorg. Chem.*, 2012, **51**, 8538–8544.
9 B. M. Flanagan, P. V. Bernhardt, E. R. Krausz, S. R. Lüthi and M. J. Riley, *Inorg. Chem.*, 2002, **41**, 5024–5033.

10 M. Kofu, O. Yamamuro, T. Kajiwara, Y. Yoshimura, M. Nakano, K. Nakajima, S. Ohira-Kawamura, T. Kikuchi and Y. Inamura, *Phys. Rev. B: Condens. Matter Mater. Phys.*, 2013, **88**, 064405.
11 K. S. Pedersen, L. Ungur, M. Sigrist, A. Sundt, M. Schau-Magnussen, V. Vieru, H. Mutka, S. Rols, H. Weihe, O. Waldmann, L. F. Chibotaru, J. Bendix and J. Dreiser, *Chem. Sci.*, 2014, **5**, 1650–1660.
12 M. E. Boulon, G. Cucinotta, J. Luzon, C. Degl'Innocenti, M. Perfetti, K. Bernot, G. Calvez, A. Caneschi and R. Sessoli, *Angew. Chem., Int. Ed.*, 2013, **52**, 350–354.
13 G. Cucinotta, M. Perfetti, J. Luzon, M. Etienne, P. E. Car, A. Caneschi, G. Calvez, K. Bernot and R. Sessoli, *Angew. Chem., Int. Ed.*, 2012, **51**, 1606–1610.
14 J. J. Baldoví, J. J. Borras-Almenar, J. M. Clemente-Juan, E. Coronado and A. Gaita-Ariño, *Dalton Trans.*, 2012, **41**, 13705–13710.
15 L. F. Chibotaru and L. Ungur, *J. Chem. Phys.*, 2012, **137**, 064112.
16 C. Görller-Walrand and K. Binnemans, in *Handbook on the Physics and Chemistry of Rare Earths*, ed. K. A. Gschneidner and L. Eyring, Elsevier, Amsterdam, 1996, vol. 23.
17 N. Magnani, R. Caciuffo, E. Colineau, F. Wastin, A. Baraldi, E. Buffagni, R. Capelletti, S. Carretta, M. Mazzera, D. T. Adroja, M. Watanabe and A. Nakamura, *Phys. Rev. B: Condens. Matter Mater. Phys.*, 2009, **79**, 104407.
18 N. Ishikawa, *Struct. Bonding*, 2010, **135**, 211–228.
19 J. Dreiser, K. S. Pedersen, C. Piamonteze, S. Rusponi, Z. Salman, M. E. Ali, M. Schau-Magnussen, C. A. Thuesen, S. Piligkos, H. Weihe, H. Mutka, O. Waldmann, P. Oppeneer, J. Bendix, F. Nolting and H. Brune, *Chem. Sci.*, 2012, **3**, 1024–1032.
20 P. Fulde, in *Handbook on the Physics and Chemistry of Rare Earths*, ed. K. A. Gschneidner Jr and E. LeRoy, Elsevier, 1979, vol. 2, pp. 295–386.
21 D. Bloor and G. M. Copland, *Rep. Prog. Phys.*, 1972, **35**, 1173–1264.
22 S. Haas, E. Heintze, S. Zapf, B. Gorshunov, M. Dressel and L. Bogani, *Phys. Rev. B: Condens. Matter Mater. Phys.*, 2014, **89**, 174409.
23 M. Moussavi, A. Decian, J. Fischer and R. Weiss, *Inorg. Chem.*, 1988, **27**, 1287–1291.
24 N. Koike, H. Uekusa, Y. Ohashi, C. Harnoode, F. Kitamura, T. Ohsaka and K. Tokuda, *Inorg. Chem.*, 1996, **35**, 5798–5804.
25 C. Benelli and D. Gatteschi, *Chem. Rev.*, 2002, **102**, 2369–2387.
26 N. Ishikawa, M. Sugita, T. Okubo, N. Tanaka, T. Lino and Y. Kaizu, *Inorg. Chem.*, 2003, **42**, 2440–2446.
27 N. Ishikawa, M. Sugita, T. Ishikawa, S. Koshihara and Y. Kaizu, *J. Phys. Chem. B*, 2004, **108**, 11265–11271.
28 M. Dörfel and J. van Slageren, unpublished work.
29 M. S. Haghighi and H. Homborg, *Z. Naturforsch., B: J. Chem. Sci.*, 1991, **46**, 1641–1649.
30 S. Stoll and A. Schweiger, *J. Magn. Reson.*, 2006, **178**, 42–55.
31 F. Aquilante, L. D. Vico, N. Ferré, G. Ghigo, P.-Å. Malmqvist, P. Neogrády, T. B. Pedersen, M. Pitonak, M. Reiher, B. O. Roos, L. Serrano-Andrés, M. Urban, V. Veryazov and R. Lindh, *J. Comput. Chem.*, 2010, **31**, 224–247.